Lower atmospheric gravity waves as sources of low-latitude traveling ionospheric disturbances as studied by an airglow imager, CHAMP satellite, and a general circulation model

Aysegul Ceren Moral[1], Kazuo Shiokawa[1], Huixin Liu[2], Shin Suzuki[3], Yuichi Otsuka[1], Clara Yoko Yatini[4] and Erdal Yigit[5]

[1] ISEE Lab, Nagoya University, Japan, [2] Dept. of Earth and Planetary Science, Faculty of Science, Kyushu University, Japan, [3] Faculty of Regional Policy, Aichi University, Japan, [4] Space Science Center, the Indonesian National Inst. of Aeronautics and Space (LAPAN), Bandung, Jawa Barat, Indonesia, [5] George Mason University, Fairfax, VA, USA

NAGOYA UNIVERSITY

ISEE 宇宙地球環境研究所 Institute for Space-Earth Environmental Research

CEDAR 2017 Workshop COUP-09

1. Abstract

Traveling ionospheric disturbances (TIDs) are studied by using three CHAMP satellite overpasses on ground-based 630-nm airglow images at low-latitudes. The airglow images are obtained from Kototabang (KTB), Indonesia (geographic coordinates: 0.2S, 100.3E, geomagnetic latitude: 10.6S). Three TID events that were simultaneously measured by the imager and CHAMP are selected for further investigation: April 30, 2006 (event 1), September 28, 2006 (event 2) and April 12, 2004 (event 3). All events show southward-moving structures in airglow images. The events 1 and 2 are single pulse events with horizontal scales of ~500-1000 km and event 3 show five wavefronts with horizontal scale sizes of 500-1000 km. For events 1 and 3, the neutral density in CHAMP shows out-of-phase variations with the airglow intensity, while event 2 is in-phase. For event 1, the relation between electron density and airglow intensity is out of phase, while the relationship between electron density and airglow intensity enhancement of event 2 and 3 are unclear, which implies that ionospheric plasma variation is not the cause of the observed TIDs. If gravity waves in the thermosphere are the source of the observed TIDs, in-phase and out-of-phase relationships of neutral density and airglow intensity can be explained by different vertical wavelengths of the gravity wave. We estimate possible vertical wavelengths for those events using observed wave parameters and modeled neutral winds. Finally, we further study the event 1 by using a general circulation model that incorporates the whole atmosphere nonlinear gravity wave scheme of Yiğit et al. (2008) and demonstrate that direct gravity propagation from the lower atmosphere to thermosphere can appreciably contribute to the observed airglow intensity enhancements. Based on these investigations, we conclude that internal gravity waves are the cause of the observed TIDs.

2. Introduction & Data

Travelling ionospheric disturbances (TIDs) are the **wave-like features** in the ionosphere.

- Typical scale size between 100 and 1000 km : medium-scale TIDs (MSTIDs),
- Typical scale size more than 1000 km : large-scale TIDs (LSTIDs) (Hunsucker, 1982)

They are **widely studied** by using many instruments: airglow imagers, ionosondes, radars, GPS systems, etc.

However the source of those disturbances has not fully been understood yet. Two main sources of TIDs; **gravity waves in the thermosphere** (Hines 1960, Hunsucker 1982) and **plasma instabilities in the ionosphere** (Miller et al. 1997, Shiokawa et al. 2003)

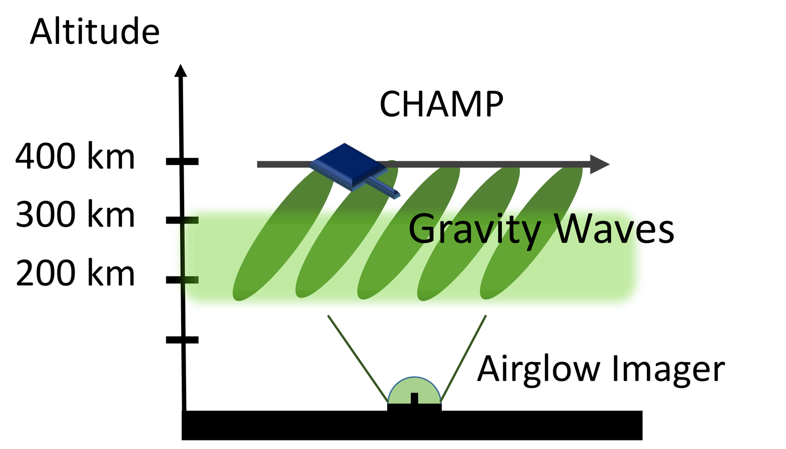

KTB station, Indonesia

- geographic coordinates: 0.2S, 100.3E,
- geomagnetic latitude: 10.6S,
- local time: UT+7 hours.

Airglow images

630-nm wavelength (OI),
emission altitude between 200 km and 300 km,
2-D images,

CHAMP satellite

Used **neutral density** and electron density data,
~400 km,
In-situ measurements,

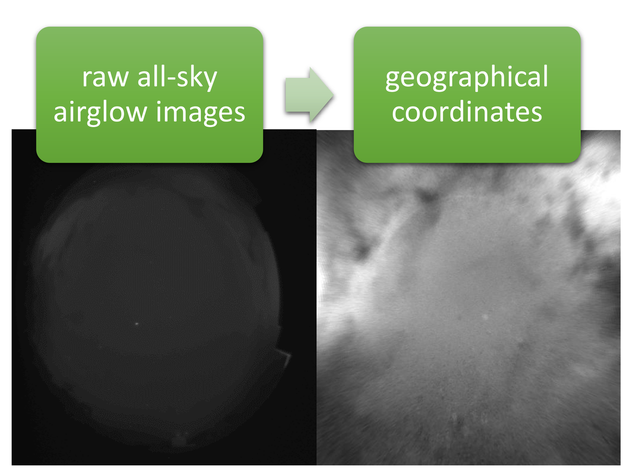

✓ percentage deviation image

$$I_d = 100 * \left(\frac{I - I_a}{I_a}\right)$$

1-hr running averages (I_a)
center image (I)

However there are no **conjugate studies** of ground airglow imager and the CHAMP satellite. Purpose of this study is understand the **GWs and their penetration** to the thermosphere and ionosphere.

3. Event 1: April 30, 2006

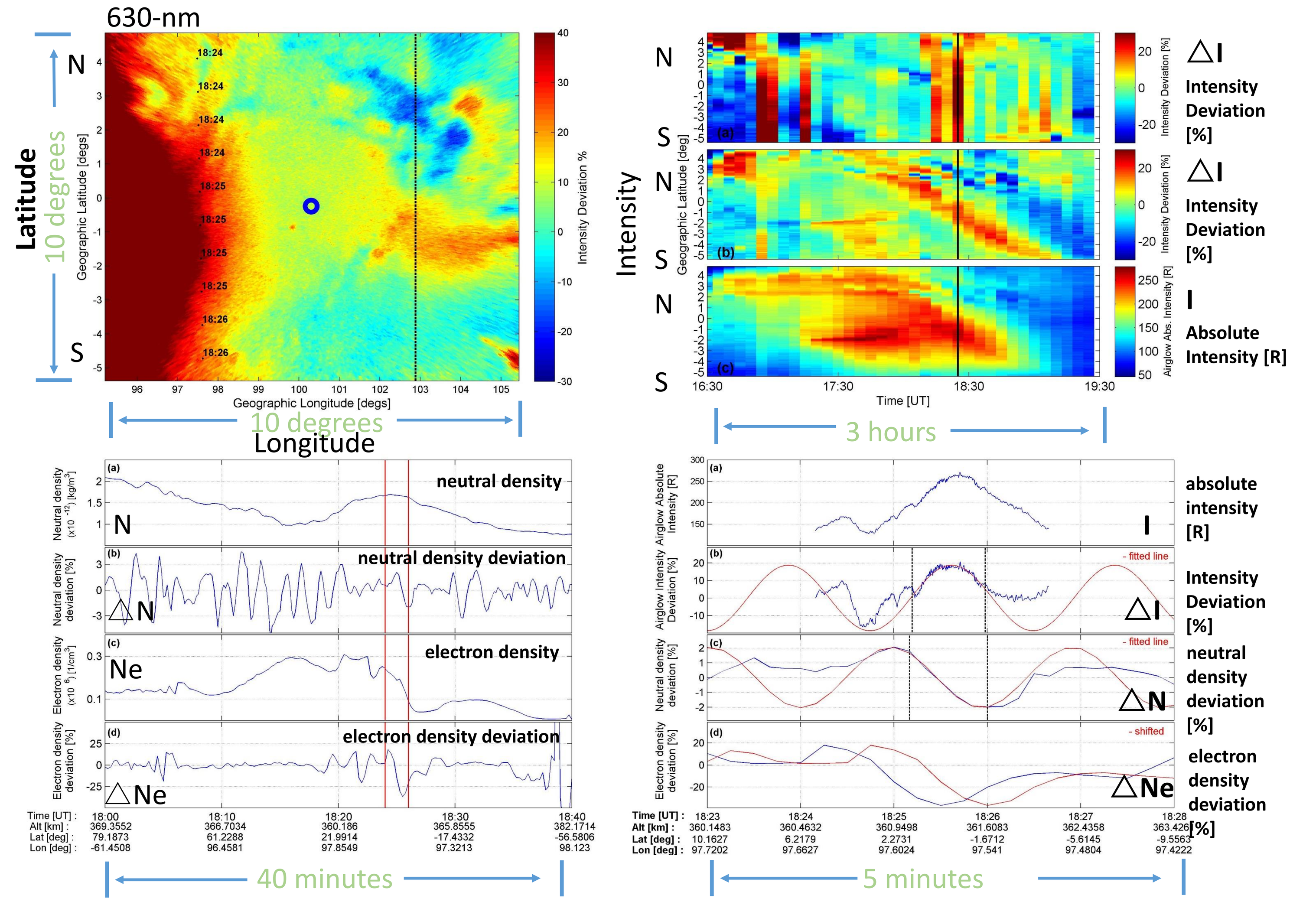

Fig. 1 – Top left panel: Airglow Image, CHAMP passage is shown with black dots and the timestamp, blue circle is KTB station, dashed black line is where the keogram (top right panel (b)) is taken. Top right panel: (a) contaminated keogram along CHAMP, (b) non-contaminated keogram along dashed black line in top left panel, (c) absolute intensity, black line indicate CHAMP passage time. Bottom left: (a) neutral density, (b) neutral density deviation, (c) electron density, (d) electron density deviation by CHAMP, red lines indicate CHAMP passage over KTB station. Bottom right: (a) absolute intensity, (b) intensity deviation, (c) neutral density deviation, (d) electron density deviation, red line on (b) and (c) are fitted lines for the data input between dashed black line is the same panel, red line in (d) indicate shifted electron density deviation along the magnetic field lines from CHAMP altitude to airglow altitude.

- The airglow image at the time when CHAMP was over KTB **at 18:26UT (01:26LT)**
- CHAMP is moving from northern hemisphere to southern hemisphere.
- Wave passage is clear on keogram however due to the contamination we could not used the data along CHAMP.

From the keogram

- north-south **scale size** of approximately **700 km**
- from 1730 UT to 1900 UT
- **southward velocity** of the wave to be ~ **106 m/s.**

- Deviations **120 s running averages** → corresponding to the horizontal scale size of 1000 km by the satellite motion.
- A clear enhancement of the airglow intensity, corresponding to the southward moving wave.
- **Sinusoidal fitting gives frequencies as 0.007 and 0.008 between airglow enhancement and CHAMP neutral density deviation. Calculated phase difference is 93 degrees.**
- **Likely to be MBW**

4. Event 2: September 28, 2006

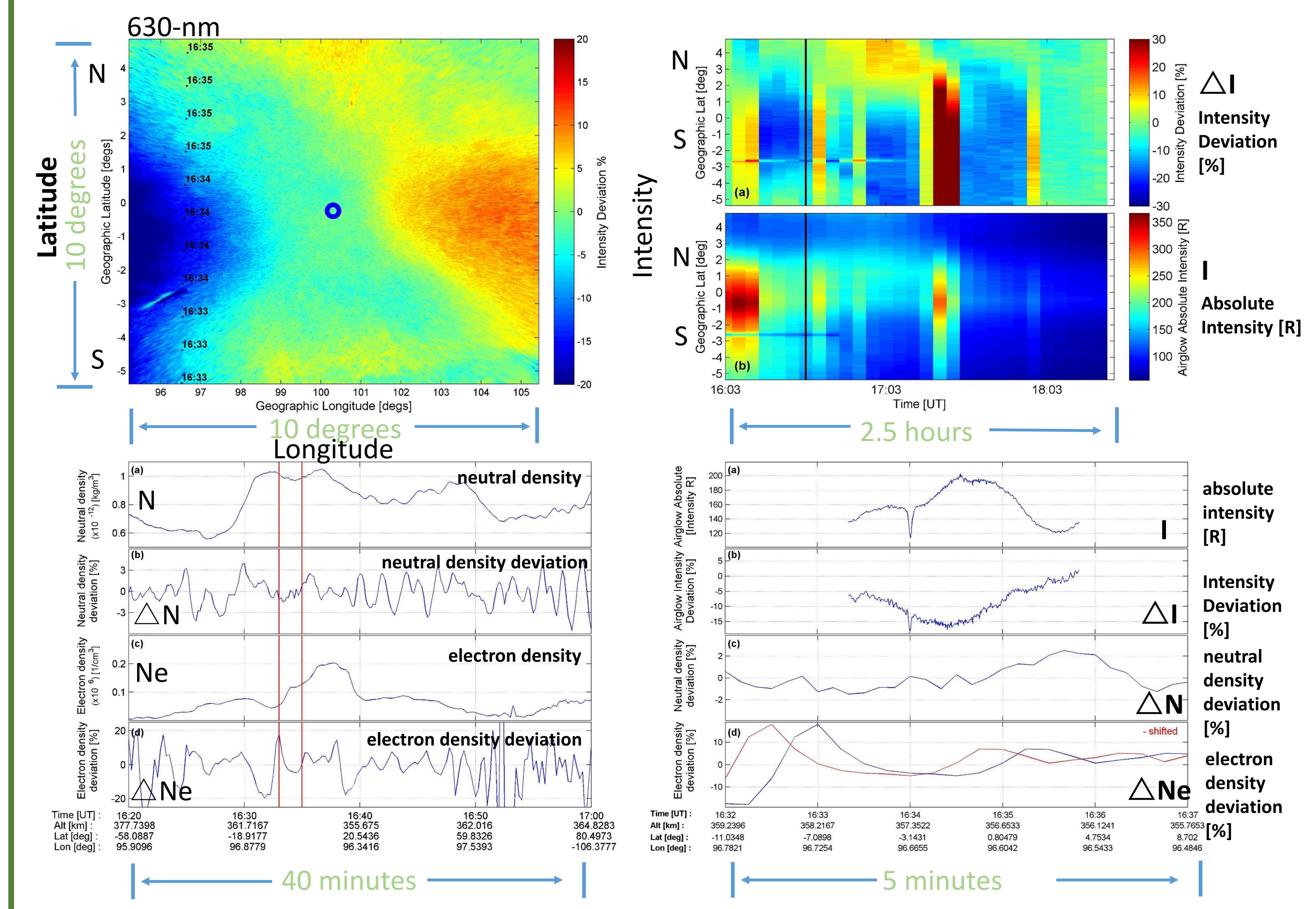

Fig. 2 – Top left panel: Airglow Image, CHAMP passage is shown with black dots and the timestamp, blue circle is KTB station. Top right panel: (a) keogram along CHAMP, (b) absolute intensity, black line indicate CHAMP passage time. Bottom left: (a) neutral density, (b) neutral density deviation, (c) electron density, (d) electron density deviation by CHAMP, red lines indicate CHAMP passage over KTB station. Bottom right: (a) absolute intensity, (b) intensity deviation, (c) neutral density deviation, (d) electron density deviation, red line (d) indicate shifted electron density deviation along the magnetic field lines from CHAMP altitude to airglow altitude.

- The airglow image at the time when CHAMP was over KTB at **16:33 UT (23:33 LT)**
- CHAMP is moving from southern to northern hemisphere .

From the keogram

- **500 km scale size** and moving southward
- from 1610 UT to 1730 UT
- southward velocity of the wave **~139 m/s.**

- **Sinusoidal fitting did not worked for this event.**
- **Neutral density deviations shows in-phase relation with airglow. However electron density deviations not show clear correspondence to the enhancement in the airglow.**
  - **→No correspondence indicates plasma instability is not the source of the waves.**
- **Likely to be MBW**

5. Event 3: April 12, 2004

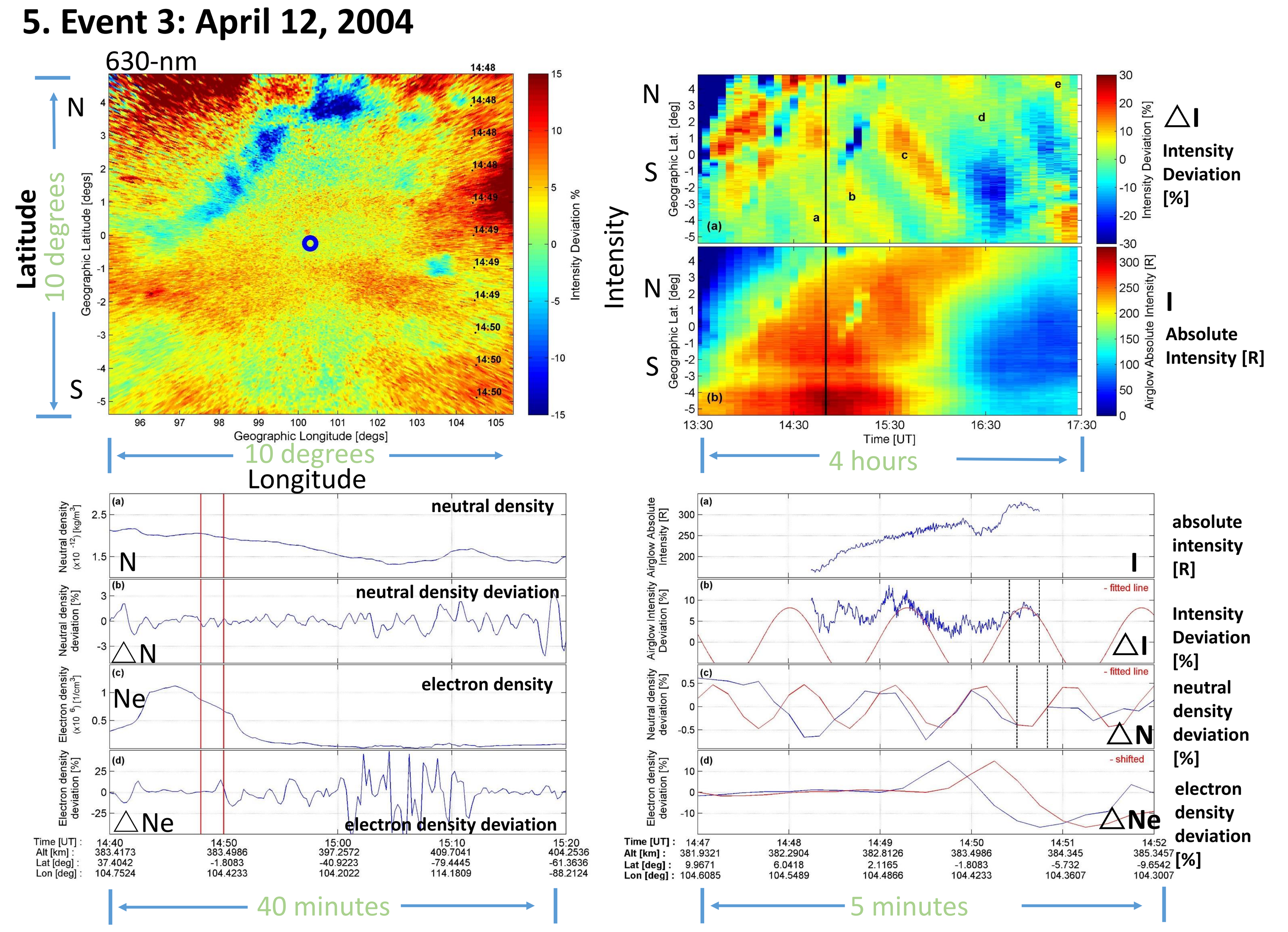

Fig. 3 – Top left panel: Airglow Image, CHAMP passage is shown with black dots and the timestamp, blue circle is KTB station. Top right panel: (a) keogram along CHAMP, (b) absolute intensity, black line indicate CHAMP passage time, wavefronts in (a) marked with letters a to e. Bottom left: (a) neutral density, (b) neutral density deviation, (c) electron density, (d) electron density deviation by CHAMP, red lines indicate CHAMP passage over KTB station. Bottom right: (a) absolute intensity, (b) intensity deviation, (c) neutral density deviation, (d) electron density deviation, red line on (b) and (c) are fitted lines for the data input between dashed black line is the same panel , red line on (d) indicate shifted electron density deviation along the magnetic field lines from CHAMP altitude to airglow altitude.

- The airglow image at the time when CHAMP was over KTB at **14:49 UT (21:49 LT)**
- CHAMP is moving from southern to northern hemisphere .

From the keogram

- Horizontal wavelengths are **500 km and 700 km** between the wave fronts
- moving southward
- southward velocity of the wave **~280 m/s.**

- **Sinusoidal fitting gives frequencies as 0.011 and 0.015 between airglow enhancement and CHAMP neutral density deviation. Calculated phase difference is 190 degrees.**
- **Electron density deviations not show clear correspondence to the waves in the airglow and neutral density deviations.**
  - **→No correspondence indicates plasma instability is not the source of the waves.**
- **Likely to be caused by MSTID**

6. Results & Discussion

1) **Sinusoidal fitting** of y=A sin(ωx + ϕ) to check the frequency component and phase difference, where A, ω and ϕ are amplitude, frequency and phase, respectively. If the frequency components are the same, we consider that it is the same wave observed in both measurements.

- For event 1 frequency is 0.007 and 0.008 rad/km for enhancement in the airglow data and CHAMP neutral density deviation, respectively. Calculated phase difference between both observation is 93 degrees.
- For event 2 sinusoidal fitting method did not worked. Visually observed phase difference between the airglow data and CHAMP neutral density deviation is in-phase.
- For event 3 frequency is 0.011 and 0.015 rad/km for enhancement in the airglow data and CHAMP neutral density deviation, respectively. Calculated phase difference between both observation is 190 degrees.

2) Linear **dispersion relationship of gravity waves** (Hines, 1960) must be satisfied by the observed waves. Then we can calculate the vertical wavelengths as:

$$\left(\frac{2\pi}{\lambda_z}\right)^2 = m^2 = \frac{N^2}{(u-c)^2} - k^2 - \frac{1}{4H^2}$$

model — model — observation

where
m = vertical wavenumber
k = horizontal wavenumber
N = Brunt-Vaisala frequency
U = background neutral wind
C = horizontal phase velocity of the waves
H = scale height

3) There is no measurements of background wind by CHAMP, so we used HMW07 model background wind velocity results in dispersion relationship. Background wind given as ±200 m/s and HMW07 model data range showed between red lines.

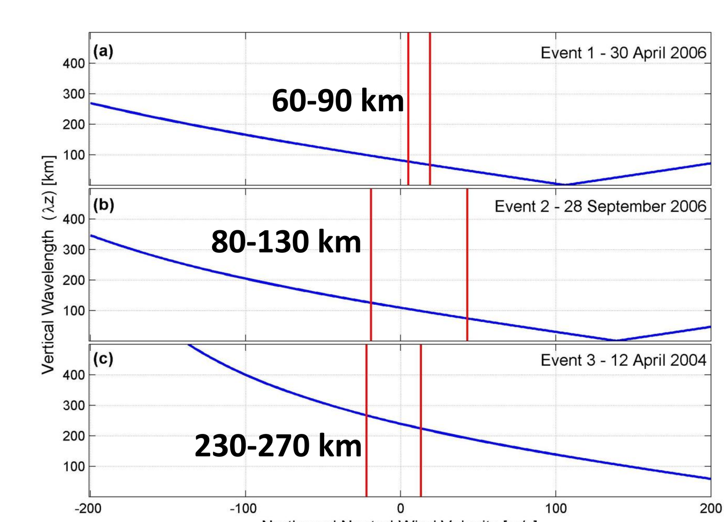

Fig. 4. Calculated vertical wavelengths for event 1 (a), 2 (b) and 3 (c). Red lines indicate the HMW07 model wind range for each event.

Calculated vertical wavelengths from dispersion relationship and ϕ are given in the table 1. For event 1, 2 and 3, the calculated vertical wavelengths are 60-90 km, 80-130 km and 230-270 km, respectively. Expected vertical wavelengths from ϕ for event 1 and 3 are 67.25 and 308 km, respectively. They are consistent with each other for event 1 and 3. Vertical wavelength calculated from dispersion relation is also consisted with observed phase differences for event 2 between airglow emission at 250 km and the CHAMP satellite neutral density measurements at 400 km.

7. Summary

Table 1. Scale size, propagation direction, apparent velocities, causes, relationship between airglow enhancement and neutral density and electron density deviations, calculated vertical wavelengths, calculated horizontal wavelengths and phase differences for event 1, 2 and 3.

	Scale size [km]	Movement	Velocity [m/s]	Cause	Ne-airglow	λ_z from dispersion [km]	Horizontal Wavelength [km]	Phase diff [deg]	λ_z from ϕ [km]
Event 1	700	Southward	106	MBW	Out-of-phase	60-90	800	93	67.25
Event 2	500	Southward	139	MBW	-	80-130	-	In-phase	-
Event 3	500-700	Southward	280	MSTID	-	230-270	560	190	308

1. Wave properties of the events are given in Table 1 as a summary.
2. Unclear relation between electron densities and airglow enhancements → plasma instability is not the source of the observed TIDs.
3. Corresponding structure between enhancement in the airglow and CHAMP neutral density deviations.
4. Calculated vertical wavelengths for all events are consisted with calculated phase differences (for event 1 and 3) and visually estimated phase relation (for event 2). → **Gravity waves are the reason of the observed TIDs**

References

- Hines, C., O. (1960), Internal atmospheric gravity waves at ionospheric heights, *Can. J. Phys*., 38, 1441-1481.
- Hunsucker, R. D. (1982), Atmospheric gravity waves generated in the high-latitude ionosphere: A review, *Rev. Geophys. Space Phys*., 20, 293-315.
- Miller, C. A., W. E. Swartz, M.C. Kelley, M. Mendillo, D. Nothingham, J. Scali, and B. Reinisch (1997), Electrodynamics of midlatitude spread F:1. Observations of unstable, gravity wave-induced ionospheric electric fields at tropical latitudes, *J. Geophys. Res*, 102(A6), 11,521-11,532, doi:10.1029/96JA03839.
- Shiokawa, K., Y. Otsuka, C. Ihara, T. Ogawa, and F. J. Rich (2003), Ground and satellite observations of nighttime medium-scale travelling ionospheric disturbance at midlatitude, *J. Geophys. Res*., 108(A4), 1145, doi:10.1029/2002JA009639.
- Yigit, E., Aylward, A.D., Medvedev, A.S. (2008), Parameterization of the effects of vertically propagating gravity waves for thermosphere general circulation models: Sensitivity study, *Journal Of Geophysical Research-atmospheres,* 113(D19),D19106, doi: 10.1029/2008JD010135.

Acknowledgement

We thank Y. Katoh, M. Satoh, Y. Yamamoto and Y. Hamaguchi of the Institute for Space-Earth Environmental Research Laboratory (ISEE), Nagoya University, for their helpful support in the all-sky imager at Kototabang. ISEE, the Research Institute for Sustainable Humanosphere, Kyoto University, Japan, and the National Institute of Aeronautical and Space Science, Indonesia were carried out airglow observations at Kototabang. We want to thank to Space Agency of the German Aerospace Center (DLR) and the project director H. Luhr for the CHAMP mission. This work was supported by Grant-in-Aids for Scientific Research (13573006, 20244080, 15H05815), on Priority Area (764), and JSPS Core-to-Core Program, B. Asia-Africa Science Platforms. Huixin Liu is supported by JSPS KAKENHI grant 15K05301, 15H02135, and 15H03733. Aysegul Ceren Moral is supported by research scholarship of the Ministry of Education, Culture, Sports, Science and Technology, Japan.